



RESEARCH LETTER

10.1002/2015GL066754

Key Points:

- Large uncertainties exist in estimating differences in split/displacement impacts in reanalyses
- Differences in annular mode responses to split and displacement SSWs are not robust across definitions
- The tropospheric impact of SSWs is strongly related to their persistence in the lower stratosphere

Supporting Information:

- Supporting Information S1

Correspondence to:

A. C. Maycock,
earamay@leeds.ac.uk

Citation:

Maycock, A. C., and P. Hitchcock (2015), Do split and displacement sudden stratospheric warmings have different annular mode signatures?, *Geophys. Res. Lett.*, *42*, 10,943–10,951, doi:10.1002/2015GL066754.

Received 27 OCT 2015

Accepted 4 DEC 2015

Accepted article online 13 DEC 2015

Published online 23 DEC 2015

Do split and displacement sudden stratospheric warmings have different annular mode signatures?

Amanda C. Maycock^{1,2,3} and Peter Hitchcock⁴

¹Centre for Atmospheric Science, University of Cambridge, Cambridge, UK, ²National Centre for Atmospheric Science, UK, ³Now at School of Earth and Environment, University of Leeds, Leeds, UK, ⁴Department of Applied Mathematics and Theoretical Physics, University of Cambridge, Cambridge, UK

Abstract Sudden stratospheric warmings (SSWs) contribute to intraseasonal tropospheric forecasting skill due to their surface impacts. Recent studies suggest these impacts depend upon whether the polar vortex splits or is displaced during the SSW. We analyze the annular mode signatures of SSWs in a 1000 year IPSL-CM5A-LR simulation. Although small differences in the mean surface Northern Annular Mode (NAM) index following splits and displacements are found, the sign is not consistent for two independent SSW algorithms, and over 50 events are required to distinguish the responses. We use the wintertime correlation between extratropical lower stratospheric wind anomalies and the surface NAM index as a metric for two-way stratosphere-troposphere coupling and find that the differences between splits and displacements, and between classification methodologies, can be simply understood in terms of their mean stratospheric wind anomalies. Predictability studies should therefore focus on understanding the factors that determine the persistence of these anomalies following SSWs.

1. Introduction

Major sudden stratospheric warmings (SSWs) are associated with rapid and large amplitude excursions in the wintertime stratospheric flow. Many studies have shown that on average following an SSW there is a negative Northern Annular Mode (NAM) index extending from the upper stratosphere to the surface, which persists for up to ~ 2 months [e.g., Baldwin and Dunkerton, 2001; Charlton and Polvani, 2007]. This stratosphere-troposphere dynamical coupling can provide additional intraseasonal predictability over Europe [e.g., Sigmond *et al.*, 2013].

Two recent studies analyzed reanalysis data and concluded that different types of SSW, classified as either a displaced or split polar vortex, have different impacts on Northern Hemisphere surface climate [Mitchell *et al.*, 2013, hereafter M13; Seviour *et al.*, 2013, hereafter S13]. These studies concluded that splitting events are followed by a negative surface NAM index, while displacement events show smaller surface anomalies, with a pattern that does not resemble the NAM. Nakagawa and Yamazaki [2006] also analyzed reanalysis data and found that SSWs coincident with a larger flux of wave number 2 wave activity, which is more typical of splits, were more likely to propagate into the troposphere than those with reduced wave number 2 activity. Such a dependence on event type could offer one explanation for why some SSWs appear to influence the troposphere and others do not [Gerber *et al.*, 2009]. However, Charlton and Polvani [2007] (hereafter CP07) used a different algorithm to identify SSWs in reanalysis data and did not find the same difference in surface response between splits and displacements as S13 and M13 [see also Cohen and Jones, 2011]. O'Callaghan *et al.* [2014] applied a hybrid method of the CP07 algorithm to identify SSWs and the M13 algorithm to classify their type to a model simulation and found that the surface response to both types of SSW projected onto the NAM, but that the magnitude of the anomaly was larger for splits in the 0–30 day period after onset. Finally, Hitchcock and Simpson [2014] (hereafter HS14) showed that the tropospheric responses to the zonally symmetric component of the vortex evolution following a split and displacement SSW were largely indistinguishable in a model experiment.

The apparent discrepancies between past studies of the surface impacts of splits and displacements in reanalysis data are related to differences in the events identified by the SSW algorithms used. While the mean SSW frequencies for the methods are broadly similar [Butler *et al.*, 2015], only $\sim 50\%$ of the onset dates found by S13 are consistent with M13 (to within ± 20 days). A similar fraction of SSW dates are consistent between CP07

and M13 (see M13 for details). Thus, conclusions about the relative impacts of split and displacement SSWs on the troposphere have been based on different samples of events. However, it is not yet clear which SSW classification methodology is most relevant for the subsequent evolution of the troposphere. Furthermore, since the reanalysis only covers a relatively short period, it is difficult to assess on the basis of these data alone whether the classification algorithms capture fundamentally different coupling behavior, or if the differences are sampling issues due to the relatively small number of SSWs. The aim of this study is to provide a more rigorous statistical analysis of the annular mode signatures of SSWs and their dependence on event type. This is achieved using a 1000 year simulation from a stratosphere-resolving climate model, to which the CP07 and S13 algorithms, and their classifications as a split or displacement, are applied.

2. Methods

Data are used from a 1000 year preindustrial control simulation from the IPSL-CM5A-LR model taken from the Fifth Coupled Model Intercomparison Project (CMIP5) archive [Taylor *et al.*, 2012]. The atmospheric component is a high-top version of the LMDZ5A model, with 39 vertical levels, a model lid at 0.04 hPa, and a $3.75^\circ \times 1.875^\circ$ lon/lat grid [Dufresne *et al.*, 2013]. The atmospheric model is coupled to the NEMO v3.2 ocean with 31 vertical levels and a horizontal resolution of 2° refined to 0.5° in the tropics. Daily data are used on eight pressure levels extending from the surface to the midstratosphere (1000, 850, 725, 500, 250, 100, 50, and 10 hPa).

Two SSW algorithms are employed in the study: the definition of CP07 based on a reversal of the daily zonal mean zonal wind (\bar{u}) at 10 hPa and 60°N to easterly during winter months, including a further classification as a split or displacement based on absolute vorticity (see CP07 for details; the change to the parameter n_c discussed by Hitchcock *et al.* [2013a] is also used here), and the definition of S13 based on 2-D moment analysis.

The use of 2-D moment analysis to study the polar vortex was first discussed by Waugh [1997] and Waugh and Randel [1999] and has been recently revisited by Mitchell *et al.* [2011]. The method of S13 describes the geometry of the polar vortex using 10 hPa geopotential height. A similar analysis was conducted by M13 using potential vorticity. In Cartesian coordinates (obtained through a Lambert equal-area azimuthal projection), the 2-D moment of order $a + b$ is calculated as

$$\mu_{ab} = \iint_S [\Phi(x, y) - \bar{\Phi}] x^a y^b dx dy,$$

where $\bar{\Phi}$ is the geopotential height at the vortex edge, taken as the climatological December to March (DJFM) zonal mean geopotential height at 60°N and 10 hPa, and S is the area enclosed by the geopotential height contour equal to $\bar{\Phi}$. The zeroth and first order moments represent the latitude of the center of the vortex and its aspect ratio; thresholds for these two moments are used to identify displacement and split SSWs, respectively. Higher order moments, such as kurtosis, are not used.

Since the frequency of SSWs in the IPSL-CM5A-LR model is around two thirds of that in reanalysis data [Charlton-Perez *et al.*, 2013], the identification thresholds are adjusted such that the 3.5% most equatorward daily values of centroid latitude, and the largest 3.5% of aspect ratio values, are captured; these are roughly two thirds of the respective fractions of 5.7% and 5.2% captured in reanalysis data by S13. The thresholds used here are as follows: the centroid latitude must be less than 66.5°N for at least seven consecutive days to define a displacement event and the aspect ratio of the vortex must be larger than 2.8 for at least seven consecutive days to define a split event. These can be compared to the equivalent thresholds of 66°N and 2.4 used in S13. However, the qualitative conclusions are similar if the S13 thresholds are used for the model (not shown).

For consistency with S13, SSWs are identified only from December to March for both algorithms. This additional constraint excludes 26 (of 271) displacement and 5 (of 167) split model SSWs identified in November by the CP07 algorithm; however, the conclusions are not sensitive to the inclusion of these additional events.

Following S13, the model is compared to a combined European Centre for Medium Range Weather Forecasts reanalysis data set consisting of ERA-40 data from 1959 to 1978 [Uppala *et al.*, 2005] and ERA-Interim data from 1979 to 2009 [Dee *et al.*, 2011]. The reanalysis events for the moment-based algorithm are therefore identical to those in S13 (17 displacements and 18 splits). The CP07 algorithm is also applied to the combined ERA data set and a total of 20 displacements and 15 splits are identified. The events before 2002 are consistent with those in CP07, with the exception that a single event on 28 November 1968 is excluded due to the restriction to DJFM.

The evolution of the atmosphere around SSWs is presented in terms of the Northern Annular Mode (NAM) index. The NAM is the leading mode of variability in the Northern Hemisphere extratropical wintertime circulation and is defined here as the leading empirical orthogonal function of Northern Hemisphere (20–90°N) daily 3-D (longitude-latitude-time) geopotential height anomalies from the climatological seasonal cycle on pressure levels [see, e.g., Baldwin and Dunkerton, 2001]. The NAM index is normalized to have unit variance and the results are therefore expressed as standard deviations. Although the NAM captures only around one third of the total daily hemispheric variance in the troposphere, it explains a much larger fraction of the mean tropospheric circulation anomalies following SSWs (HS14) [O'Callaghan *et al.*, 2014]. However, HS14 also showed that the zonal mean response to SSWs includes a smaller easterly anomaly poleward of 65°N, which does not project onto the NAM. Since the analysis here focuses on the leading modes of variability, the non-NAM component of the response will not be discussed further; however, we note that this is a less studied aspect of the response to SSWs which warrants further investigation.

3. Results

Charlton-Perez *et al.* [2013] showed that the IPSL-CM5A-LR model has a relatively low SSW frequency ($\sim 4.5 \text{ decade}^{-1}$) compared to other models with a well-resolved stratosphere (based on the CP07 definition). Figure 1a shows the frequency of split (red) and displacement (blue) SSWs in the combined ERA reanalysis data and the IPSL-CM5A-LR model for the S13 and CP07 algorithms. The whiskers show 95% confidence intervals estimated using the method of Hitchcock *et al.* [2013a], which assumes that the occurrence of SSWs follows a binomial distribution. Consistent with the findings of Charlton-Perez *et al.* [2013], there are $\sim 35\%$ fewer SSWs in the model compared to the reanalysis. The overall SSW frequencies are similar for the two methods, with the exception that CP07 identifies slightly fewer splits in the model. Despite the mean SSW frequency being lower than observed, the climatological zonal mean zonal wind and its interannual variability in the Arctic winter stratosphere is comparable to the reanalysis, with the main difference being that the modeled winds are too strong by $\sim 10 \text{ m s}^{-1}$ at 10 hPa and by $\sim 5 \text{ m s}^{-1}$ at 100 hPa from February onward (see supporting information Figure S1).

Figures 1b and 1c show the seasonal distributions of SSWs in the model for the S13 and CP07 algorithms, respectively. The crosses denote the respective values for the ERA reanalysis. The confidence intervals for each algorithm overlap in all months, indicating that there are no distinguishable differences in the monthly mean frequencies of splits or displacements identified by the two methods. However, the S13 algorithm identifies more splits than displacements in January, and vice versa in March. The CP07 algorithm also identifies more displacements than splits in March and in February.

Figures 1d and 1e show time-log pressure composites of the NAM index around SSWs identified by the S13 algorithm for (d) the IPSL-CM5A-LR and (e) the ERA reanalysis. Similar results are obtained for the CP07 algorithm (not shown). Despite the overall SSW frequency being lower in the model, the mean NAM signature is broadly comparable to the reanalysis data. There are two main exceptions: first, the stratospheric anomalies associated with SSWs appear to persist for ~ 30 days longer in the model than in the reanalysis. While the factors that determine this bias are of interest [e.g., Hitchcock *et al.*, 2013b], the focus here is on the 1–2 month time scale where the differences in the NAM between the model and reanalysis are less pronounced. Second, the NAM index in the midtroposphere is possibly less negative in the model from around 10 days after the SSW onset, though the uncertainties in the detailed evolution of the reanalysis composite are substantial. The processes that determine the vertical structure of stratosphere-troposphere coupling are also an active research topic [e.g., Garfinkel *et al.*, 2013], which goes beyond the scope of this study; however, the magnitudes of the near-surface NAM index, which is the focus of this study, are comparable in the model and reanalysis. The spatial structure and internal variability of the near-surface NAM index are also comparable for the model and reanalysis (see supporting information Figure S2).

The numbers in parentheses in Figures 1b and 1c denote the number of SSWs identified in the model. The large number of events enables an assessment of the robustness of the estimated NAM response for small sample sizes, such as those found in reanalyses. A Monte Carlo repeat sampling (10^5 times) is conducted to estimate the confidence intervals for the difference in the 30–60 day averaged 1000 hPa NAM index following splits and displacements as a function of SSW sample size. The results are shown in Figure 2 for the (a) S13 and (b) CP07 algorithms. Since the variance of the large-scale monthly mean circulation in the Northern

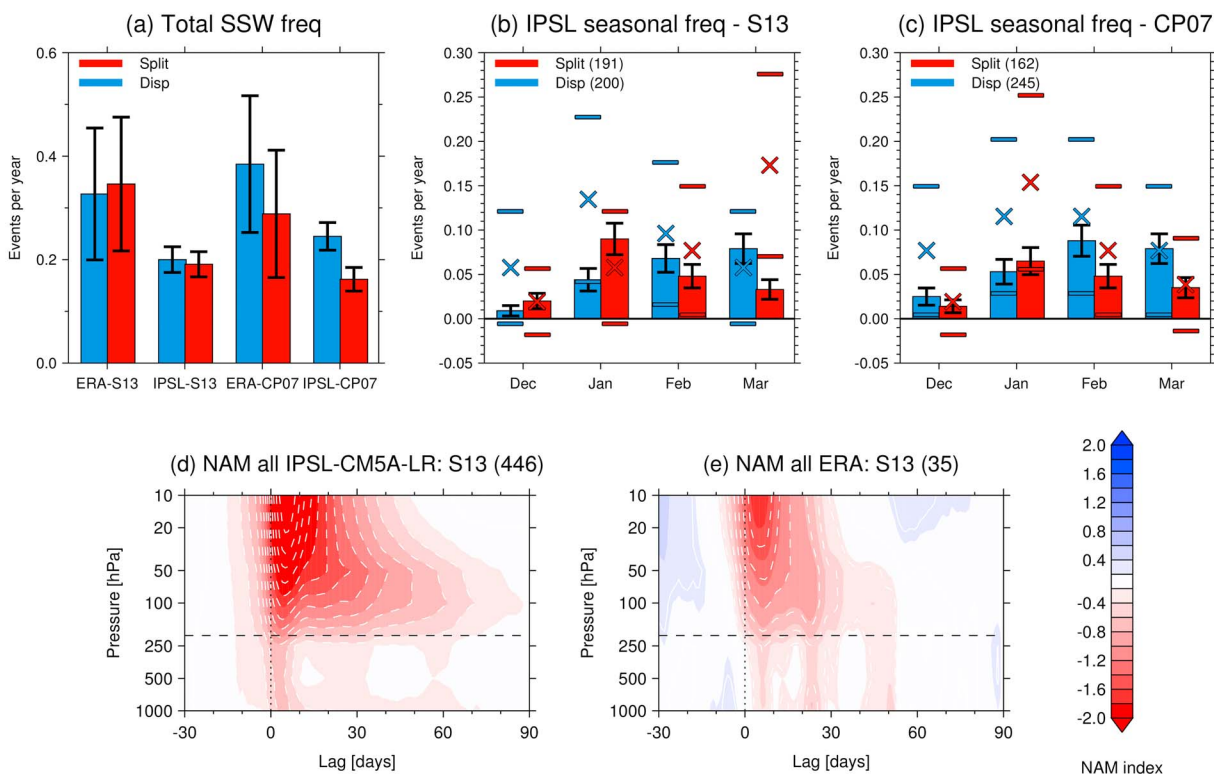


Figure 1. (a) The total frequency of SSWs in the ERA reanalysis and the IPSL-CM5A-LR model for the S13 and CP07 definitions. The whisker plots show 95% confidence intervals. (b, c) The seasonal distribution of SSWs in the 1000 year IPSL-CM5A-LR model for the S13 and CP07 definitions, respectively. Blue (red) bars show displacement (split) events. The whisker plots show 95% confidence intervals. The crosses in Figures 1b and 1c show the corresponding frequencies in the ERA reanalysis data, and the thick colored dashes denote the 95% confidence intervals on these values. (d) Composite lag-height plots of the Northern Annular Mode (NAM) index for all modelled SSWs identified by the S13 algorithm. White contours denote ± 0.2 intervals in the NAM index, values between ± 0.2 are not shaded. (e) As in Figure 1d but for the ERA reanalysis data. The values in brackets indicate the total number of SSWs in each category.

Hemisphere troposphere is comparable in the model and reanalysis (see supporting information Figure S2), there is no a priori reason to suspect that the estimated uncertainties are significantly biased.

The differences in the mean 1000hPa NAM index between splits and displacements in the reanalysis data (black diamonds) are (1) not of the same sign for the two SSW algorithms and (2) not highly statistically significant according to the confidence intervals estimated from the model. Similar results are found for the 0–30 day period (see supporting information Figure S3). Although M13 stated that the 15–45 day averaged 1000 hPa NAM index following splits was greater than two standard deviations from the mean, whereas for displacements it was not, they did not discuss the significance of the difference in the NAM index between the two types of SSW. Figure 2 shows that this difference is not highly significant for either algorithm given the number of SSWs currently represented in reanalyses.

Figure 3 shows that composites of 18 SSWs, the approximate number of each type in the reanalysis, can be found from the model in which both splits and displacements either do or do not show a tropospheric NAM signal up to 2 months after the event onset. These can be compared to similar plots for the reanalysis shown in Figure 4 of M13. The composites represent the (a, c) 10th and (b, d) 90th percentiles of the 30–60 day 1000 hPa NAM index following (a, b) displacements and (c, d) splits. These results emphasize that the tropospheric signature associated with a small number of SSWs may not be representative of a larger sample.

The conclusions from Figure 2 are broadly consistent with the analysis of sea level pressure fields by M13, which revealed only small regions where the surface responses to splits and displacements were found to be statistically significantly different using a Student's *t* test (see their Figure 7i). For reference, stereographic maps of the mean sea level pressure anomalies averaged over 0–30 and 30–60 days after SSW onset are shown for the ERA reanalysis and IPSL-CM5A-LR model in supporting information Figures S4–S7.

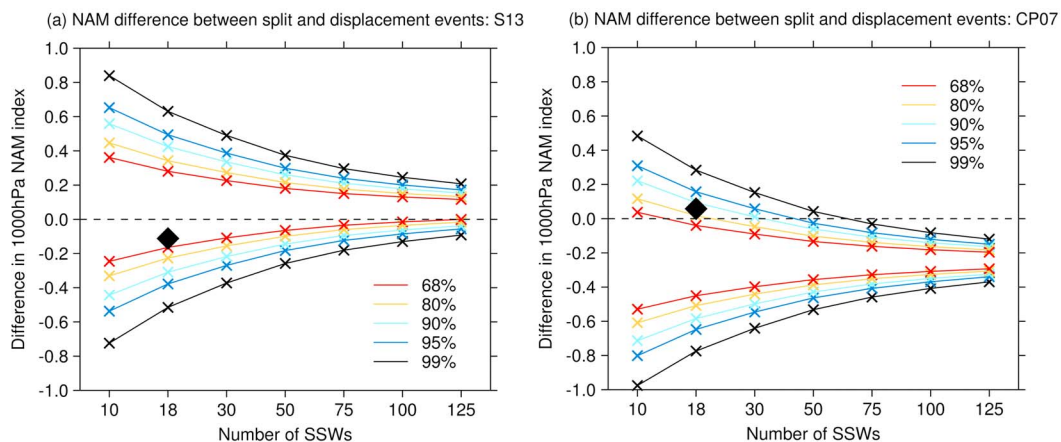


Figure 2. Confidence intervals for the difference in 30–60 day mean 1000 hPa NAM between split and displacement SSW events as a function of sample size. The estimates have been constructed using a Monte Carlo repeat sampling (10^5 times) of SSW events from a 1000 year control integration of the IPSL-CM5A-LR model. SSWs are identified using the (a) S13 and (b) CP07 definition. The black diamond denotes the difference in the mean 1000 hPa NAM between displacements and splits in the ERA reanalysis data set.

In the limit of a large number of SSWs in the model, Figure 2 does show significant differences in the mean 1000 hPa NAM index between splits and displacements for the CP07 algorithm. In this case, the mean NAM indices across all modeled events are -0.45 and -0.21 for splits and displacements, respectively, implying a stronger surface response following splits. However, for the S13 algorithm, the corresponding values of -0.28 and -0.34 are not found to be significantly different (see also supporting information Table S1). Note that in the CP07 case, at least ~ 50 events of each type are required to identify a difference in the near-surface NAM index that is statistically significant at the 95% confidence level; this is around 3 times the number in current reanalyses.

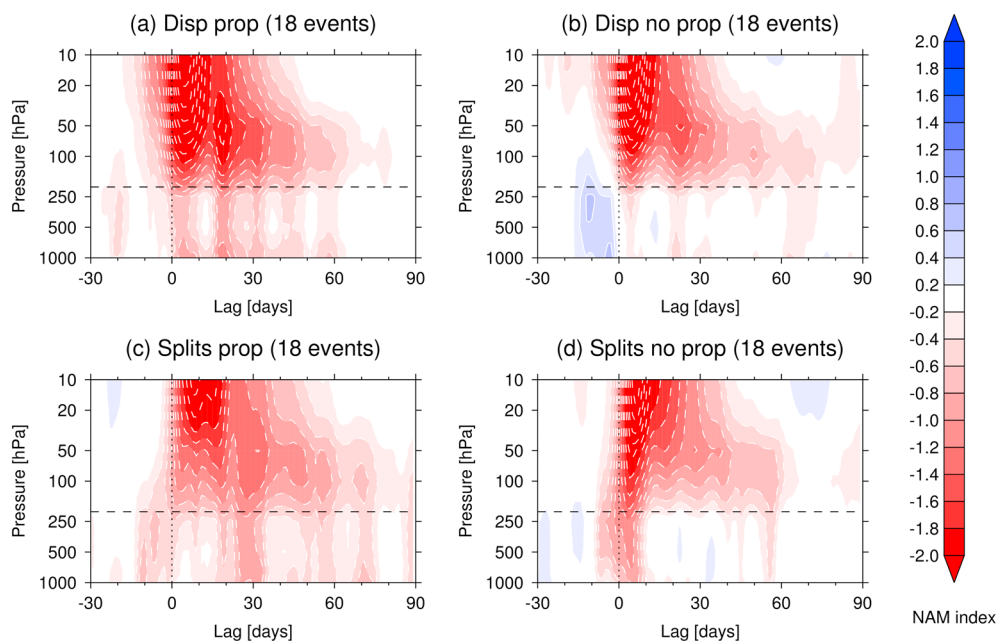


Figure 3. Composite lag-height plots of the Northern Annular Mode (NAM) index for four sets of 18 SSW events from the IPSL-CM5A-LR model categorized as (a, b) displacement and (c, d) split events. The white contours denote ± 0.2 intervals in the NAM index, values between ± 0.2 are not shaded. Figures 3a and 3c show persistent negative NAM anomalies in the troposphere; Figures 3b and 3d show a weaker tropospheric response.

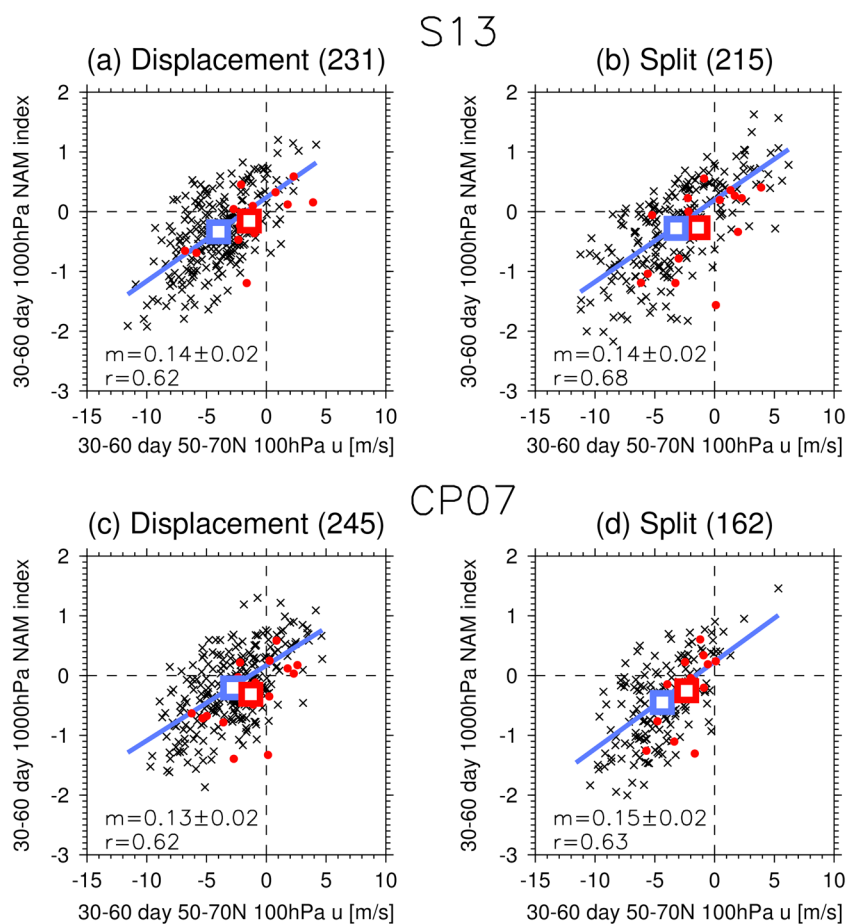


Figure 4. Scatterplots of the 30–60 day mean 50–70°N \bar{u} at 100 hPa (ms^{-1}) versus the 30–60 day mean 1000 hPa NAM index following SSW events in the IPSL-CM5A-LR model (black crosses) and the ERA reanalysis data (red circles). The squares denote the averages of all the points for the model (blue) and reanalysis (red). Data are shown for (a, c) displacements and (b, d) splits for the (a, b) S13 and (c, d) CP07 algorithms. The blue lines show linear regressions for each set of model points with slope, m , and $\pm 2\sigma$ uncertainty range and Pearson correlation coefficient, r , given in the legend.

Figure 2 also shows that the difference in the 1000 hPa NAM index between splits and displacements depends upon the identification method employed (see also supporting information Figure S3 for 0–30 days). While it is possible that the two algorithms detect different dynamical behavior, which could explain the contrasting responses, they have, in principle, been designed to capture the same phenomena. Since there is no consensus around the optimum metric for identifying SSWs and their type [Butler *et al.*, 2015], it is not yet clear which method provides greatest insight into stratosphere-troposphere coupling. We therefore seek a more general means of assessing stratosphere-troposphere coupling in the model and reanalysis.

Figure 4 shows scatterplots of the 30–60 day mean 50–70°N \bar{u} anomaly at 100 hPa versus the 30–60 day mean 1000 hPa NAM index following SSWs. The 100 hPa \bar{u} anomaly is used as a measure of the magnitude and persistence of the SSW in the extratropical lower stratosphere, but qualitatively similar results are found using polar cap mean 100 hPa geopotential height (not shown). The four panels in Figure 4 show (a, c) displacement and (b, d) split events for the (a, b) S13 and (c, d) CP07 algorithms. The black crosses show individual SSWs from the model and the blue lines show linear regressions fitted to these points. The red circles show equivalent events from the reanalysis. The colored squares denote the averages of the model and reanalysis samples.

There is a significant correlation between the extratropical lower stratospheric wind anomalies and the 1000 hPa NAM index; in all cases, the Pearson correlation coefficient for the model data is 0.62–0.68. Note that this is similar to the correlation found if data from all winter months are included (supporting information Figure S8a) [see also Baldwin and Thompson, 2009], so this can be seen as a metric for the two-way coupling

between the stratosphere and troposphere. It is not possible to discern from this relationship alone the relative contributions from upward and downward effects, and we do not attempt to do so here [see, e.g., Siegmund, 2005]. However, stratospheric anomalies following SSWs have been shown to impact on the near-surface NAM index [e.g., HS14; Hitchcock *et al.*, 2013a], and these anomalies are, in general, larger and more persistent than those at other times. The correlation in Figure 4 therefore implies that the corresponding tropospheric anomalies are also larger and more persistent following SSWs. The correlation between the stratospheric winds and surface across all winter months diminishes with increasing height but is still significant at 10 hPa given the large number of data points in the model (see supporting information Figures S8b and S8c). The relationship in winter is different from that in summer months (see supporting information Figure S9), which might be expected given the dependence of the processes that determine stratosphere-troposphere dynamical coupling (such as Rossby wave propagation and breaking) on the seasonal cycle.

In Figure 4 there is considerable spread of points about the lines of best fit for all four SSW classifications; this reinforces the conclusion from Figures 2 and 3 that mean responses for small numbers of SSWs have substantial uncertainties due to internal atmospheric variability. The reanalysis events also lie within the modeled distributions, providing further evidence that the representation of stratosphere-troposphere coupling following SSWs is comparable in the model and reanalysis up to 2 months after the onset (see also supporting information Figure S10). Presenting the data in this way also highlights that the number of each category of SSW in the reanalysis undersamples the true population distribution of the \bar{u} /NAM phase space, estimated here using the model data; as noted earlier, this is a significant source of uncertainty. Similar results are found for the 0–30 day period following SSWs (see supporting information Figure S10).

A key finding from Figure 4 is that there are no significant differences in the slopes of the regressions for split and displacement SSWs, which might be expected if the two-way stratosphere-troposphere coupling captured by this metric varied with SSW type. There are also no significant differences in the regression slopes between the S13 and CP07 algorithms. Across both split and displacement events for the CP07 algorithm, the values of the regression slopes are 0.13 ± 0.07 for the ERA reanalysis and 0.14 ± 0.02 for the IPSL-CM5A-LR model. It would appear that this slope is an important property for a model to quantitatively capture and may be a useful benchmark for models. With regard to the mean location of events in the \bar{u} /NAM phase space, for the CP07 algorithm, a greater fraction of splits have more negative stratospheric \bar{u} anomalies than for displacements, and the mean NAM index is also more negative. For the S13 algorithm, the average stratospheric anomalies following splits and displacements are more similar, but slightly larger for displacements, and the NAM index anomaly is correspondingly also more negative, although this difference is not highly statistically significant (see supporting information Table S1). The results suggest that, rather than focusing solely on SSW type, improving our understanding of the factors that determine the amplitude and persistence of circulation anomalies in the lower stratosphere may offer a more robust approach for leveraging additional skill in forecasting the NAM index following SSWs.

4. Discussion

Recent studies using reanalysis data have suggested that the tropospheric response to SSWs depends upon the type of event, categorized as either a vortex split or displacement [Mitchell *et al.*, 2013; Seviour *et al.*, 2013] (M13 and S13, respectively). These studies found that the surface anomalies following splits project more strongly onto the Northern Annular Mode (NAM) than for displacement events. This is in contrast with Charlton and Polvani [2007] (CP07) and Cohen and Jones [2011] who did not find a consistent difference in the impact of splits and displacements using a different method for identifying SSWs.

This study assesses the NAM signatures of split and displacement SSWs using a 1000 year simulation from the IPSL-CM5A-LR model and two independent algorithms for defining SSWs (those of CP07 and S13). The long integration enables a more statistically robust assessment of the role of SSW type compared to previous studies using reanalysis data. The difference in the mean surface NAM index following splits and displacements is not found to be statistically significant for the reanalysis given the small number of SSWs in the record. The contrasting conclusions of past studies of split and displacement SSWs using reanalyses are therefore likely to be subject to substantial sampling uncertainties (M13, S13, and CP07) [Cohen and Jones, 2011; Nakagawa and Yamazaki, 2006].

In the model simulation, which includes around an order of magnitude more SSWs than the reanalysis, splits are associated with a more negative near-surface NAM index than displacements for the CP07 algorithm.

The opposite appears to be the case for the S13 method, but the difference is not statistically significant despite the large number of events considered. This demonstrates that even when the sampling errors are reduced, the relative impact of splits and displacements can depend on the details of the SSW identification methodology; there is currently no consensus as to which method is most skillful at capturing stratosphere-troposphere coupling events.

Instead of focusing solely on SSW type, we propose the significant correlation between the extratropical lower stratospheric (100 hPa) zonal wind anomalies and the 1000 hPa NAM index as a useful metric for diagnosing two-way stratosphere-troposphere coupling. The \bar{u} /NAM phase space offers a useful method for framing the events captured by different SSW algorithms, since the relationship is robust across both SSW classification methodologies and both SSW types and is comparable for the model and reanalysis. The over-persistence of the stratospheric anomalies following SSWs in the model does not appear to significantly affect the relationship between the stratospheric winds and the 1000 hPa NAM index up to 2 months after the onset.

The \bar{u} /NAM relationship also suggests that the magnitude and persistence of circulation anomalies in the lowermost stratosphere is important for assessing the likelihood of there being a tropospheric signal up to 2 months after the onset of an SSW. Many model studies of stratosphere-troposphere coupling around SSWs combine the effects of possible biases or variability in the representation of stratospheric anomalies with possible biases in the representation of the underlying “strength” of stratosphere-troposphere coupling. The consistency of the \bar{u} /NAM relationship across SSWs presents an initial pathway to begin separating these components. For example, if a model simulates too weak stratospheric anomalies around SSWs, it may still produce a \bar{u} /NAM slope which compares with reanalyses. Equally, a model may simulate more realistic stratospheric variability, but the underlying \bar{u} /NAM relationship may be misrepresented. Both of these aspects are important for capturing two-way stratosphere-troposphere coupling in models and would have a quantitative impact on the regional surface responses to SSWs. Predictability studies may therefore focus on factors that determine the magnitude and persistence of a given SSW, for example, through identifying the characteristics near the onset that determine its evolution; previous work suggests this may bear some relation to SSW type [Yoden *et al.*, 1999; Hitchcock *et al.*, 2013a]. On the other hand, process studies may wish to understand the factors that determine the slope of the \bar{u} /NAM relationship; this appears to be largely independent of the SSW type and indeed may be characterizable outside of SSW periods, such as when the vortex is anomalously strong [e.g., Baldwin and Dunkerton, 2001]. Further work is required on this latter issue in particular.

Acknowledgments

A.C.M. was supported by a Postdoctoral Fellowship from the AXA Research Fund. P.H. was supported by an NSERC Postdoctoral Fellowship. A.C.M. and P.H. acknowledge support from ERC ACI grant project 267760. We thank the IPSL modeling group and the World Climate Research Programme for making the model simulation available through the CMIP5 archive and ECMWF for making available the ERA-40 and ERA-Interim reanalysis data sets. We thank William Seviour for providing the code for the 2-D moment analysis. We also thank Isla Simpson for providing useful feedback on an earlier version of the manuscript and Lorenzo Polvani for stimulating discussions. Finally, we thank the detailed comments from two anonymous reviewers which improved the manuscript.

References

- Baldwin, M. P., and T. J. Dunkerton (2001), Stratospheric harbingers of anomalous weather regimes, *Science*, *244*, 581–84.
- Baldwin, M. P., and D. W. J. Thompson (2009), A critical comparison of stratosphere-troposphere coupling indices, *Q. J. R. Meteorol. Soc.*, *135*, 1661–1672.
- Butler, A. H., D. J. Seidel, S. C. Hardiman, N. Butchart, T. Birner, and A. Match (2015), Defining sudden stratospheric warmings, *Bull. Am. Meteorol. Soc.*, doi:10.1175/BAMS-D-13-00173.1, in press.
- Charlton, A. J., and L. Polvani (2007), A new look at stratospheric sudden warmings. Part I. Climatology and modeling benchmarks, *J. Clim.*, *20*, 449–469.
- Charlton-Perez, A. J., et al. (2013), On the lack of stratospheric dynamical variability in low-top versions of the CMIP5 models, *J. Geophys. Res. Atmos.*, *118*, 2494–2505, doi:10.1002/jgrd.50125.
- Cohen, J., and J. Jones (2011), Tropospheric precursors and stratospheric warmings, *J. Clim.*, *24*, 1780–1790, doi:10.1029/2008JD010623.
- Dee, D. P., et al. (2011), The ERA-Interim reanalysis: Configuration and performance of the data assimilation system, *Q. J. R. Meteorol. Soc.*, *137*(656), 553–597.
- Dufresne, J.-L., et al. (2013), Climate change projections using the IPSL-CM5 Earth System Model: From CMIP3 to CMIP5, *Clim. Dyn.*, *40*, 2123–2165.
- Garfinkel, C. I., D. W. Waugh, and E. P. Gerber (2013), The effect of tropospheric jet latitude on coupling between the stratospheric polar vortex and the troposphere, *J. Clim.*, *26*, 2077–2095.
- Gerber, E. P., C. Orbe, and L. M. Polvani (2009), Stratospheric influence on the tropospheric circulation revealed by idealized ensemble forecasts, *Geophys. Res. Lett.*, *36*, L24801, doi:10.1029/2009GL040913.
- Hitchcock, P., and I. Simpson (2014), The downward influence of sudden stratospheric warmings, *J. Atmos. Sci.*, *71*, 3856–3876.
- Hitchcock, P., T. G. Shepherd, and G. L. Manney (2013a), Statistical characterization of Arctic polar-night jet oscillation events, *J. Atmos. Sci.*, *70*, 2096–2116.
- Hitchcock, P., T. G. Shepherd, M. Taguchi, S. Yoden, and S. Noguchi (2013b), Lower-stratospheric radiative damping and polar-night jet oscillation events, *J. Atmos. Sci.*, *70*, 1391–1408.
- Mitchell, D. M., A. J. Charlton-Perez, and L. J. Gray (2011), Characterizing the variability and extremes of the stratospheric polar vortices using 2D moment analysis, *J. Atmos. Sci.*, *68*, 1194–1213.
- Mitchell, D. M., L. J. Gray, J. Anstey, M. P. Baldwin, and A. J. Charlton-Perez (2013), The influence of stratospheric vortex displacements and splits on surface climate, *J. Clim.*, *26*, 2668–2682.
- Nakagawa, K. I., and K. Yamazaki (2006), What kind of stratospheric sudden warming propagates to the troposphere?, *Geophys. Res. Lett.*, *33*, L04801, doi:10.1029/2005GL024784.

- O'Callaghan, A., M. M. Joshi, D. Stevens, and D. M. Mitchell (2014), The effects of different sudden stratospheric warming types on the ocean, *Geophys. Res. Lett.*, *41*, 7739–7745, doi:10.1002/2014GL062179.
- Seviour, W. J. M., D. M. Mitchell, and L. J. Gray (2013), A practical method to identify displaced and split stratospheric polar vortex events, *Geophys. Res. Lett.*, *40*, 5268–5273, doi:10.1002/grl.50927.
- Siegmund, P. (2005), Stratospheric polar cap mean height and temperature as extended-range weather predictors, *Mon. Weather Rev.*, *133*, 2436–2448.
- Sigmond, M., J. F. Scinocca, V. V. Kharin, and T. G. Shepherd (2013), Enhanced seasonal forecast skill following stratospheric sudden warmings, *Nat. Geosci.*, *6*, 98–102.
- Taylor, K. E., R. J. Stouffer, and G. A. Meehl (2012), An overview of CMIP5 and the experiment design, *Bull. Am. Meteorol. Soc.*, *93*, 485–498.
- Uppala, S. M., P. W. Kållberg, A. J. Simmons, U. Andrae, V. D. C. Bechtold, M. Fiorino, J. K. Gibson, J. Haseler, A. Hernandez, and G. A. Kelly (2005), The ERA-40 re-analysis, *Q. J. R. Meteorol. Soc.*, *131*(612), 2961–3012.
- Waugh, D. W. (1997), Elliptical diagnostics of stratospheric polar vortices, *Q. J. R. Meteorol. Soc.*, *123*, 1725–1748.
- Waugh, D. W., and W. J. Randel (1999), Climatology of Arctic and Antarctic polar vortices using elliptical diagnostics, *J. Atmos. Sci.*, *56*, 1594–1613.
- Yoden, S., T. Yamaga, S. Pawson, and U. Langematz (1999), A composite analysis of the stratospheric sudden warmings simulated in a perpetual January integration of the Berlin TSM GCM, *J. Meteorol. Soc. Jpn.*, *77*, 431–445.